Geophysical Journal International

Geophys. J. Int. (2010) **183,** 79–95 doi: 10.1111/j.1365-246X.2010.04735.x

Lithospheric density variations and Moho structure of the Irish Atlantic continental margin from constrained 3-D gravity inversion

J. Kim Welford,[1] Patrick M. Shannon,[2] Brian M. O'Reilly[3] and Jeremy Hall[1]

[1] *Department of Earth Sciences, Memorial University of Newfoundland, St. John's, NL, Canada. E-mail: kwelford@mun.ca*
[2] *UCD School of Geological Sciences, University College Dublin, Belfield, Dublin 4, Ireland*
[3] *Dublin Institute for Advanced Studies, 5 Merrion Square, Dublin 2, Ireland*

Accepted 2010 July 10. Received 2010 July 6; in original form 2009 August 25

SUMMARY

A 3-D density anomaly model of the Irish Atlantic continental margin was generated from a regional inversion of the free air gravity data constrained by bathymetric and sediment thickness information. The model results are compared against a recent regional Moho structure compilation from velocity models from crustal-scale wide-angle reflection/refraction surveys. Using the inverted model, a regional map of Moho structure across the margin agrees well with the regional seismic compilation and also provides information in areas lacking deep seismic coverage. The density anomaly structure of the crust across the margin is investigated along model slices and using volume rendering of crustal layers. These views reveal extreme thinning of the upper crust and a dominance of lower crustal densities in regions where exhumation of serpentinized mantle has previously been interpreted. Using the regional view afforded by the inversion, the areal extent of these zones is tracked into regions lacking seismic constraints. Using the regional density anomaly model, variations in sediment thickness and crustal thickness are investigated to compute stretching factors across the margin and to identify zones which deviate from local isostatic compensation. These zones generally correlate with faults and rifting trends providing insights that could be useful for future palaeoreconstructions of North Atlantic rifting.

Key words: Inverse theory; Gravity anomalies and Earth structure; Continental margins: divergent; Continental tectonics: extensional; Crustal structure; Atlantic Ocean.

1 INTRODUCTION

The separation of Ireland and Newfoundland during the opening of the modern North Atlantic Ocean began in the Late Cretaceous (de Graciansky & Poag 1985; Tucholke *et al.* 1989; Hopper *et al.* 2006; Tucholke & Sibuet 2007) and has been interpreted by Doré *et al.* (1999) as an oblique re-opening of the Caledonian–Appalachian suture and fold system. This NE–SW striking suture and fold system developed due to the closing of the Iapetus Ocean in Palaeozoic time which stitched together the distinct basement terranes that make up the offshore Irish and Newfoundland margins (Haworth & Keen 1979; Williams 1984, 1995). The broad basement affinities of these margins have been deduced from geological provenance studies (Lilly 1965; King *et al.* 1985; Tyrrell *et al.* 2007) and regional seismic compilations (Hall *et al.* 1998) and clear linkages across the conjugate margin pair are apparent (Fig. 1).

The modern Irish Atlantic region (Fig. 2A) consists of a wide passive margin with a complicated tectonic history involving the overprinting of Late Palaeozoic to Cenozoic extension and inversion on the older basement terranes. The cumulative effect of these events, and their resultant structures, played a major role in influencing the location, orientation and history of the younger sedimentary basins that lie in the offshore. As some of the larger basins are lightly explored but potentially petroliferous, an enhanced regional knowledge of the nature and structure of the underlying crust is needed. Seismic profiling has been undertaken across many parts of the margin but due to variable data quality and vintages, understanding of the overall geological basement and crustal structure remains poor.

A better regional understanding of the margin can be obtained using a 3-D inversion of gravity data that integrates existing geological and geophysical information and extrapolates these to provide information on unsampled regions. The aim of this paper is to present the results of such a study on the structurally complex, Irish Atlantic continental margin. The inverted results allow for the identification of Moho, crustal and sediment variations across the rifted margin. These provide new constraints on the regional North Atlantic evolution and basin development.

2 CRUSTAL STRUCTURE AND DEVELOPMENT

Closure of the Iapetus Ocean in late Silurian times led to the Caledonian orogeny resulting from the docking and suturing of the distinct basement terranes that make up the Irish offshore margin. By Late

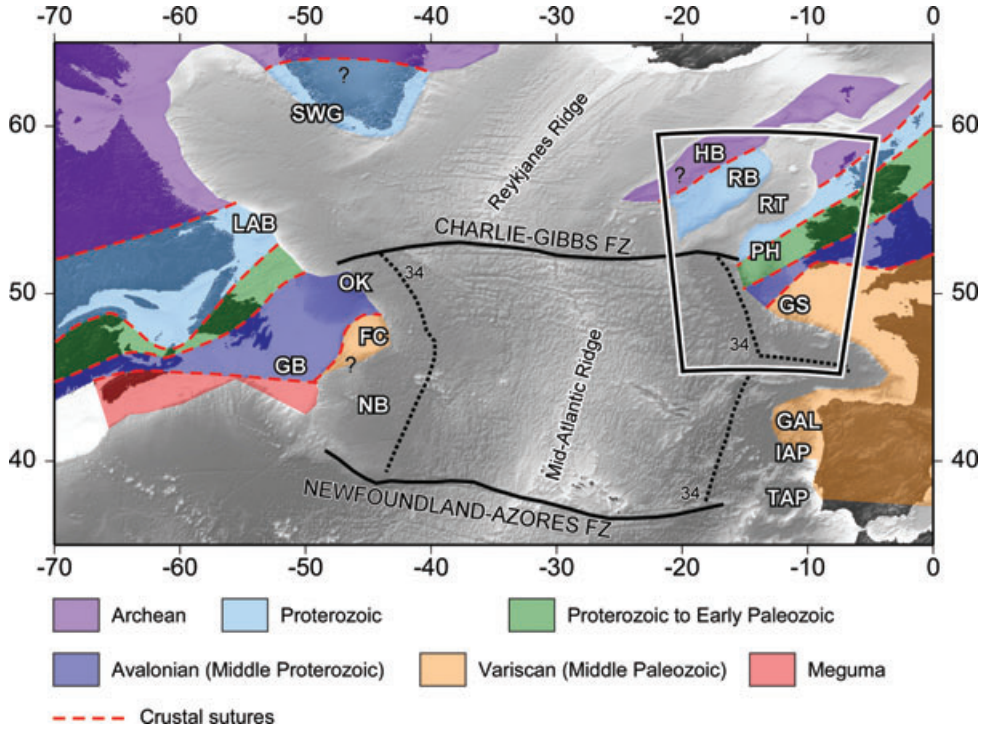

Figure 1. Bathymetric map of the North Atlantic region subdivided by inferred basement affinity of continental crust, adapted from Hall *et al.* (1998) and Tyrrell *et al.* (2007). The black box outlines the study region and the area used for the constrained 3-D gravity inversion. Location of magnetic anomaly 34 (from Srivastava *et al.* 1988a,b, 1990) is plotted as dotted line segments. Bathymetric structure abbreviations: FC, Flemish Cap; FZ, Fracture Zone; GAL, Galicia Bank; GB, Grand Banks; GS, Goban Spur; HB, Hatton Bank; IAP, Iberian Abyssal Plain; LAB, Labrador; NB, Newfoundland Basin; OK, Orphan Knoll; PH, Porcupine High; RB, Rockall Bank; RT, Rockall Trough; SWG, South West Greenland; TAP, Tagus Abyssal Plain.

Carboniferous times, an east-west trending fabric was superimposed on the basement of the Irish continental margin by northward migration of deformation from the Variscan orogeny to the south (Landes *et al.* 2005). Further deformation was imposed from Late Palaeozoic to Cenozoic time as the margin underwent multiple extension and rifting events which caused the development of a number of offshore basins whose geometry was controlled largely by pre-existing basement structures and tectonic fabrics (Shannon 1991). Separation of the Irish continental margin from its conjugate pair, the northern Flemish Cap/Orphan Basin region of Newfoundland, Canada, occurred during the Late Cretaceous (Tucholke *et al.* 1989; Hopper *et al.* 2006).

The Mesozoic basins and the continent–ocean margin in this region are typically parallel to the NE–SW Caledonian structures although basement fabric in onshore Ireland changes to an ENE–WSW alignment towards the south coast where Caledonian and Variscan fabrics are sub-parallel. This orientation is evident in the North Celtic Basin where the ENE–WSW orientation either reflects a strike swing in the Caledonian fabric, or a Variscan structure (or possibly a combination with a Caledonian structure that was reactivated in Variscan times). The ENE–WSW fabric is also seen in the eastern part of the Goban Spur province and in the orientation of the Porcupine Fault at its northern margin (Fig. 2A; Naylor *et al.* 2002; Naylor & Shannon 2005).

The unstretched crust beneath Ireland is approximately 30 km thick (Lowe & Jacob 1989; Hauser *et al.* 2008), while beneath the Irish and Celtic Sea regions it is approximately 25 km thick, with evidence of crustal decoupling to accommodate the slight thinning beneath the basins (O'Reilly *et al.* 1991). The nature and the thickness of the crust beneath the large Atlantic basins such as the Porcupine and Rockall basins has been the subject of considerable debate (see Smythe Smythe 1989; Shannon *et al.* 1999). However, robust geophysical evidence from the RAPIDS (Rockall And Porcupine Irish Deep Seismic) profiles indicates the presence of severely thinned continental crust beneath the largest basins, intruded locally by mantle serpentinites or volcanics (Makris *et al.* 1988, 1991; Hauser *et al.* 1995; O'Reilly *et al.* 1996; Reston *et al.* 2001; O'Reilly *et al.* 2006). The continental crust beneath the centres of the Rockall and Porcupine basins is 2–5 km thick and is interpreted to have undergone differential stretching, with greater upper and middle crustal extension facilitated by rheologically controlled detachments at the top of the lower crust.

The thickness of the crust on the continental shelf has been well constrained by deep-seismic profiles (Morewood *et al.* 2005; O'Reilly *et al.* 2006). Recent studies onshore (van den Berg *et al.* 2005; Hauser *et al.* 2008) have suggested that the main phase of crustal accretion and growth occurred during the Caledonian orogenic cycle. However, little else is known about the composition or detailed nature of the crust or its age. Naylor & Shannon (2005) identified several distinct basement (pre-Permian) provinces in the Porcupine-Rockall region, based on seismic character and on the structure of the overlying basin sediments. Rockall Bank is thought to belong to the Islay (Rockall Bank basement) terrane, with the boundary against Lewisian rocks lying to the north, in UK waters (Hitchen *et al.* 1997). Geological provenance analysis (Tyrrell *et al.* 2007) suggests the existence of Archaean, Proterozoic, Avalonian and Variscan domains extending through the offshore region (Fig. 1).

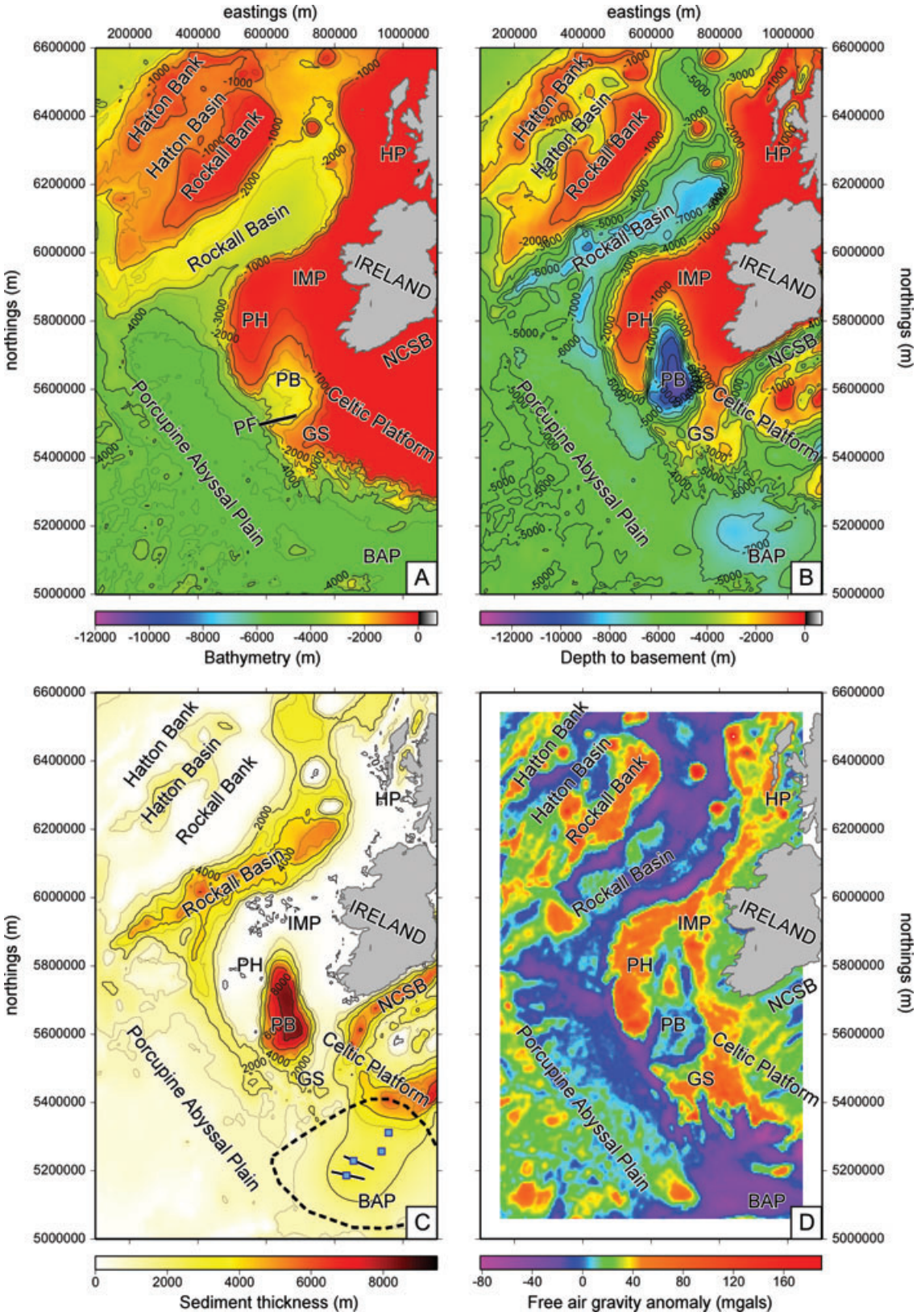

Figure 2. Maps of (A) bathymetry, (B) depth to basement, (C) sediment thickness and (D) free air gravity anomalies for the study region, the offshore Irish margin. On map (C), the dashed black line outlines an anomalously deep suspect basin in the NOAA compilation which was replaced with alternate sediment thickness constraints (shown by blue squares) from de Graciansky *et al.* (1985) and from two seismic lines from Ginzburg *et al.* (1985) which were used to interpolate across the outlined region. The location of the Porcupine Fault (PF) is shown by the thick black line on map (A). Key bathymetric structures of the margin are labelled in black on all plots. Bathymetric structure abbreviations: BAP, Biscay Abyssal Plain; GS, Goban Spur; HP, Hebridean Platform; IMP, Irish Mainland Platform; NCSB, North Celtic Sea Basin; PB, Porcupine Basin; PH, Porcupine High.

3 SEDIMENTARY BASIN ARCHITECTURE

Initial post-Variscan sedimentary basin development on the Irish margin took place in a series of localized Permian basins in the foothills of the Variscan mountains and sometimes in depocentres controlled by the gravitational collapse of Variscan orogenic structures. Early to mid Triassic depocentres were partly infilled topographic lows as well as partly rift induced (Štolfovà. & Shannon 2009). Through Late Triassic and into Early Jurassic times, localized fault-controlled depocentres developed, but deposition was largely in broad and shallow thermal subsidence depocentres. Middle Jurassic rifting followed caledonoid-oriented crustal fabrics and structures (e.g. the Celtic Sea and the Slyne-Erris basins). The onset of the north–south elongate rifts in the Porcupine Basin probably developed in Late Jurassic (Sinclair *et al.* 1994). Plate reorganization led to the development of a regional Base Cretaceous unconformity. A local phase of rifting occurred during the Aptian–Albian. Thereafter regional thermal subsidence, accompanied by a eustatic sea level rise, occurred in all the basins, giving rise to major Chalk deposition with very little terrigenous input. The Cenozoic marked a major change with a combination of basin inversion, return to clastic deposition and marked igneous activity especially in the Atlantic margin basins. Cenozoic Plate reorganizations led to large localized sediment wedges, inversion events and differential basin restructuring (Haughton *et al.* 2005; Praeg *et al.* 2005). The structure of the basins was complicated by igneous activity broadly coincident with crustal breakup along the Hatton Continental Margin (Vogt *et al.* 1998).

The precise influence of older structural fabrics on basin evolution is not well understood or straightforward. Some basins are parallel to underlying crustal fabrics while others are slightly oblique to the main structures (Fig. 2C). In yet other places, the basins bear no obvious relationship to the orientation of basement structures. Several of the rift basins on the Irish margin have been studied extensively. These include the Celtic Sea basins, the Rockall Basin and the Porcupine Basin (Naylor & Shannon 2009). While the Celtic Sea basins and the Rockall Basin have a broadly northeast–southwest Caledonian orientation, the Porcupine Basin has a north–south orientation and appears to have been more strongly influenced by east–west extension due to the opening of the North Atlantic Ocean rather than by pre-existing basement fabrics (Shannon 1991).

4 GRAVITY DATA

Free air gravity anomalies over the Irish Atlantic continental margin were obtained from the DNSC08 gravity anomaly compilation from the National Space Institute of the Technical University of Denmark (Andersen *et al.* 2008). These satellite altimetry data represent an updated and augmented version of an earlier compilation from Sandwell & Smith (1997) of the results from both the Geosat Geodetic Mission and the ERS 1 Geodetic Phase mission. This new compilation provides improved coverage for short spatial scales and for both polar and coastal regions. The data used in the inversion for this study are shown in Fig. 2(D).

Over the Irish Atlantic margin in general, strong positive free air gravity anomalies are confined to the continental shelf (Rockall Bank, Porcupine High, Celtic Platform, Hebridean Platform and Irish Mainland Platform) although there is also a major localized high in the centre of the Porcupine Basin (Naylor *et al.* 2002; O'Reilly *et al.* 2006). Meanwhile, the thinner crust beneath the Hatton Basin, the Rockall Basin and the Porcupine Abyssal Plain is characterized by gravity lows.

5 3-D GRAVITY INVERSION

This study of the Irish region follows an earlier study of the Newfoundland margin (Welford & Hall 2007) and provides complementary new results from the conjugate northwest European Atlantic margin. The aim of the regional 3-D gravity inversion was to provide large-scale depth to Moho, crustal density distribution and crustal thickness estimates across the entire Irish Atlantic continental margin using only bathymetric and sediment thickness information to constrain the inverted results. While constraints from localized seismic studies were not used to directly constrain the inversion, they were used indirectly to decide on the optimal maximum depth of the inverted mesh and were used to locally assess the success of the inversion. The basic inversion methodology and parameters are outlined below followed by descriptions of the constraining data sets and how they were incorporated into the inversion. Finally, the sources of corroborating geophysical constraints are provided.

5.1 Inversion methodology

Both this study and the complementary Newfoundland margin study (Welford & Hall 2007) employed the same inversion algorithm, GRAV3D, developed by Li & Oldenburg (1996, 1998), and the choice of model parameters is generally similar. Thus, the reader is directed to Welford & Hall (2007) for a more detailed explanation of the GRAV3D algorithm and the model parameters used.

In brief, the GRAV3D algorithm generates a subsurface 3-D density anomaly model (relative to an arbitrary reference density) by inverting gravity observations at the Earth's surface. The anomalous mass required to reproduce a given gravity anomaly is vertically distributed within the underlying model with that distribution fundamentally controlled by a depth-weighting function but also according to assigned smoothing parameters and also relative to a reference density model if one is used. For this study, a reference density anomaly model constrained by bathymetric and sediment thickness information was used, essentially forcing the inversion to distribute any remaining anomalous mass at depth beneath these two shallower prescribed layers.

When inverting surface gravity observations, the GRAV3D algorithm attempts to optimize the balance between how well the model conforms to the desired output (model norm) and how well the inverted model is able to reproduce the observations within their error bounds (misfit). Directionally dependent smoothing length scales are used to define the model norm and these can be adjusted to produce any range of model types (e.g. small, flat and blocky).

Simultaneously, the inversion tries to ensure that the gravity predictions computed from the model fit the observations as closely as possible in a least-squares sense given the errors associated with those observations. The difference between the observed and predicted gravity values is further weighted by the reciprocal of the observed data errors such that the target misfit for the inversion is dimensionless and should be equal to the number of data points provided that the data errors are independent and Gaussian with zero mean (Li & Oldenburg 1998).

With the GRAV3D algorithm, each cell within the reference density anomaly model is assigned a specific starting density anomaly and a range of density anomalies over which that density anomaly is allowed to vary during the inversion. This allows for portions of the

reference model that are well constrained from other geophysical methods to be kept fixed or only slightly varied during the inversion.

The mesh onto which the 3-D density anomaly distribution is modelled consists of rectangular prisms. These prisms can be of arbitrary size and each prism is assigned a constant density anomaly. For this study, the mesh was constructed from flattened cubes with lateral dimensions of 5 km × 5 km and 500 m thick. The horizontal extent of the mesh corresponded to the study area shown in Fig. 2 and contained 200 cells in the eastings direction and 320 cells in the northings direction.

When using the GRAV3D algorithm for constructing crustal-scale models where absolute density increases as a function of depth, the choice of the maximum mesh depth is crucial to deriving meaningful results. As demonstrated in Welford & Hall (2007) where a reference density of 2670 kg m^{-3} was used, varying the maximum mesh depth was shown to have a fundamental impact on the correspondence between interfaces derived from other geophysical methods and the equivalent ones extracted from the inverted density anomaly model. This makes intuitive sense since the anomalous mass required to reproduce a given gravity anomaly doesn't change but will be spread over fewer or more cells depending on the total depth of the mesh used. For the Newfoundland example where a reference density of 2670 kg m^{-3} was used, the best correspondence between structures resolved from the regional inversion and existing seismic constraints was obtained for a 25 km deep mesh. Subsequent to that study, tests were done to determine whether equivalently good matches with existing seismic constraints could be obtained for a deeper mesh by using a higher reference density. Tests over the Irish Atlantic margin revealed an excellent match for a 35 km deep mesh when a reference density anomaly of 2850 kg m^{-3} was used for the inversion. The remaining results presented in this paper were generated with this combination.

The gravity data used in the inversion are the free air gravity point measurements shown in Fig. 2(D). The gravity point measurements were averaged above each 5 km by 5 km mesh cell in order to reduce the number of observations used in the inversion and consequently to significantly reduce the computation time. A 60 km wide band of padding cells, corresponding to the white border in Fig. 2(D), was placed around the study area. Errors for individual gravity data point measurements were not available but the overall accuracy of the gravity anomalies was reported as ranging from 4 to 7 mGals based on comparisons with ship track data (Sandwell & Smith 1997). Since GRAV3D requires that each observation be assigned an error, an error of 5 mGals was arbitrarily chosen for each of the averaged measurements. Picking a lower error would result in a more structured model for a given misfit value.

For the inversion undertaken for this study, GRAV3D generated a 3-D density anomaly model that was smooth over length scales of 25 km in the eastings and northings directions and smooth over a length scale of 5 km in depth. Since we were trying to reproduce the long wavelength gravity anomalies using a coarse mesh, the target misfit was relaxed to two times the number of averaged data points. Test inversions using lower misfits produced geologically unreasonable (i.e. introduced high frequency structure) density anomaly models that bore less resemblance to models from complementary geophysical methods.

5.2 Constraints

Bathymetric constraints for the Irish Atlantic continental margin (Fig. 2A) were freely obtained from the General Bathymetric Chart of the Oceans (GEBCO) global 30 arc-second gridded bathymetric data set (http://www.gebco.net/data_and_products/gridded_bathymetry_data). This data set, generated primarily from quality-controlled ship depth soundings, is an interpolated data set with the interpolation guided by satellite altimetry bathymetry measurements which are not independent from the satellite gravity data used in the inversion. However, within the study area, a total of 2 931 386 depth sounding measurements are available representing over 95 per cent of the bathymetric constraints used. Consequently, the bathymetric constraints and the inverted satellite gravity data are essentially independent.

The bathymetric data for the Irish margin (Fig. 2A) were incorporated into the reference density anomaly model by forcing all model prisms above the bathymetric depths to contain density anomalies corresponding to ocean water (−1820 kg m^{-3} relative to a background density of 2850 kg m^{-3}). The density anomaly values in these prisms were kept fixed during the inversion.

Minimum sediment thickness estimates (Fig. 2C) were obtained for most of the study region from the National Geophysical Data Center (NGDC) of the National Oceanic and Atmospheric Administration (NOAA) Satellite Information Service (http://www.ngdc.noaa.gov/mgg/sedthick/). These estimates were compiled from isopach maps, ocean drilling results and seismic reflection profiles. Due to the wide range of sources and vintages of the compiled thickness estimates, quantifying errors in the data set is difficult. However, since the mesh used for the inversion is relatively coarse in depth (500 m deep cells) and provided the thickness errors are not kilometres in scale, these should have only a minor and localized impact on the inversion results. One region in the NOAA compilation where a large discrepancy was observed (outlined by the dashed line in Fig. 2C) suggested the presence of an extensive sedimentary basin with over 8 km of sediments. Since both seismic reflection profiling and drilling results from the Deep Sea Drilling Project (de Graciansky *et al.* 1985; Ginzburg *et al.* 1985) within the outlined region reveal sediment thicknesses between 2 and 3 km above basement and show no evidence of substantially thicker post-Variscan sediments, it is not clear how such a thick basin was obtained for the NOAA compilation. We therefore accepted the definitive well and seismic data, which also fitted regional sediment thickness patterns, and discounted the NOAA compilation where the thickness could not be verified. Consequently, representative sediment thicknesses were extracted from the results presented by de Graciansky *et al.* (1985) and Ginzburg *et al.* (1985) at the locations indicated by the blue squares in Fig. 2(C). These constraints were used to interpolate sediment thickness values within the outlined region. The resulting map (Fig. 2C) was then combined with the regional bathymetric data (Fig. 2A) to compute the depth to acoustic basement across the study area (Fig. 2B).

When incorporating the sediments into the reference density anomaly model, a different approach to that used in Welford & Hall (2007) was adopted. This was because preliminary inversion results over many of the deep basins showed poor matches with results from well-constrained seismic studies. In Welford & Hall (2007), the sediments were incorporated into the reference density anomaly model by assigning a density anomaly of −400 kg m^{-3} (relative to a background density of 2670 kg m^{-3}) to the prisms lying between the seabed and the basement. During the inversion, the density anomaly values within each of these prisms was then allowed to range between −600 and −200 kg m^{-3}, corresponding to a range in densities of 2070–2470 kg m^{-3}. This approach was geologically unreasonable in the present study for two reasons. First, this parametrization imposed a hard boundary at the top of the

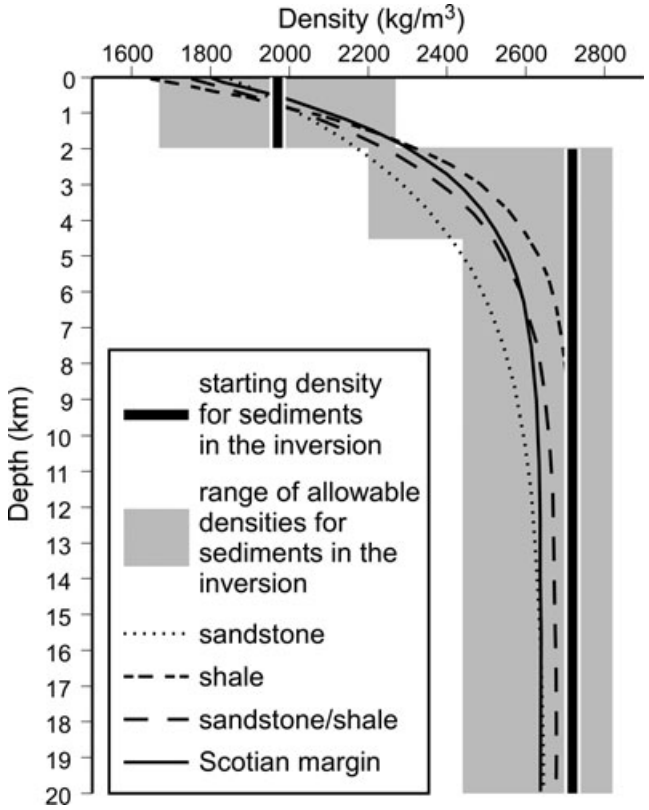

Figure 3. Plot of density versus depth for pure sandstone, for pure shale, for a sandstone and shale mix and for the average curve for the Nova Scotian margin. All curves were computed using Athy's law (Athy 1930) with the sandstone and shale constraints obtained using average trends in passive margin basins from the Gulf of Mexico (Jackson & Talbot 1986) and the North Sea (Sclater & Christie 1980). The average curve for the Scotian margin was compiled by Albertz *et al.* (2010). The thick black constant density lines show the starting density values used for sediments in the gravity inversion. The grey areas show the depth-dependent range of allowable densities for sediments in the inversion.

basement in the model and in so doing did not take into account possible errors in the regional sediment thickness estimates compiled by NOAA. Second, this parametrization did not take into account the fact that sediments within the deepest parts of the basins would be heavily compacted and so would have correspondingly higher densities, often comparable to basement rocks.

From examination of compaction curves with density as a function of depth for comparable sediments on the Nova Scotian margin (Fig. 3; Albertz *et al.* 2010), the lowest density values within the basins should occur within the top 2 km. Below that, the densities rapidly increase and approach densities typical of basement rocks. The range of possible densities for sedimentary rocks also narrows and overlaps the lower end of the range of possible densities for basement rocks. Consequently, a lower starting density anomaly of $-880\ \mathrm{kg\,m^{-3}}$ was assigned to the top 2 km of the sedimentary basins. In addition, a starting density anomaly of $-130\ \mathrm{kg\,m^{-3}}$ was assigned for deeper parts of the basins and below. While the density anomaly values within the shallow sedimentary prisms were then allowed to vary between -1180 and $-580\ \mathrm{kg\,m^{-3}}$, corresponding to densities of 1670–2270 $\mathrm{kg\,m^{-3}}$, the allowable density ranges for deeper parts of the basins were made depth dependent (Fig. 3). In this way, the sediment thickness information from the NOAA data and from de Graciansky *et al.* (1985) and Ginzburg *et al.* (1985) was used to constrain the inversion while at the same time not imposing a hard boundary at the base of the sedimentary succession. This approach also limited the negative impact of inadvertently using erroneous sediment thickness estimates in the inversion.

All prisms below the sedimentary basins within the reference density anomaly model were also assigned a starting density anomaly of $-130\ \mathrm{kg\,m^{-3}}$ so as to avoid imposing a hard boundary within the reference density anomaly model. During the inversion, the density anomaly in each of these prisms was allowed to vary between -410 and $520\ \mathrm{kg\,m^{-3}}$ (corresponding to a range in densities of 2440 to 3370 $\mathrm{kg\,m^{-3}}$). Thus, the reference density anomaly model was completely homogeneous beneath the sediments (i.e. no layering) and the inversion was given great flexibility in assigning density anomalies beneath the sediments to reproduce the observed gravity response and no constraints were placed on which prisms should correspond to crustal rocks (with density anomalies of approximately less than $170\ \mathrm{kg\,m^{-3}}$) and which prisms should correspond to upper mantle rocks (with density anomalies of approximately greater than $170\ \mathrm{kg\,m^{-3}}$).

5.3 Corroborating evidence

A recent compilation of 2-D wide-angle reflection/refraction seismic profiles for the UK, Ireland and the surrounding seas (Kelly *et al.* 2007) provides a regional view of seismic velocities and Moho depths over a large portion of NW Europe. The resulting interpolated seismic Moho map overlaps with most of our study region and provides a quasi-independent measure against which to gauge the local reliability of the inverted Moho estimates, bearing in mind that the seismic results were used to guide the choice of the maximum depth of the inverted mesh. While the Moho results from Kelly *et al.* (2007) could have been directly incorporated as constraints in the inversion, this was not done for three reasons. First, the regional Moho map from Kelly *et al.* (2007) is an interpolated map that is only as accurate as the sparse seismic constraints of varying quality and vintage used to construct it. By using them as hard constraints in the inversion, as yet seismically unsampled Moho variations could be masked and erroneously reposed as localized density variations within the crust. Second, while constraints from individual seismic lines could have been incorporated into the reference density anomaly model in GRAV3D by locally altering the inversion smoothing parameters along those lines, this approach would require the incorporation of possibly erroneous assumptions about the correspondence between velocities and densities in the region and could introduce inversion artefacts due to the variable smoothing. Third, the goal of this study was to add to the regional understanding of the margin using results from an independent and complementary method, namely constrained 3-D gravity inversion. Most recently, a study by Kimbell *et al.* (2010) involving combined regional forward gravity modelling and targeted gravity inversion of key lithospheric layers provides a new alternate source of results against which the results from this study can be compared.

5.4 Inversion results

By inverting for the averaged free air gravity data using the reference density anomaly model and the parameters outlined above, a 3-D density anomaly model was generated that was able to successfully reproduce the gravity observations along the Irish margin (Fig. 4A). All of the main observed gravity features are reproduced and the magnitudes of the gravity field values match well. Some horizontal

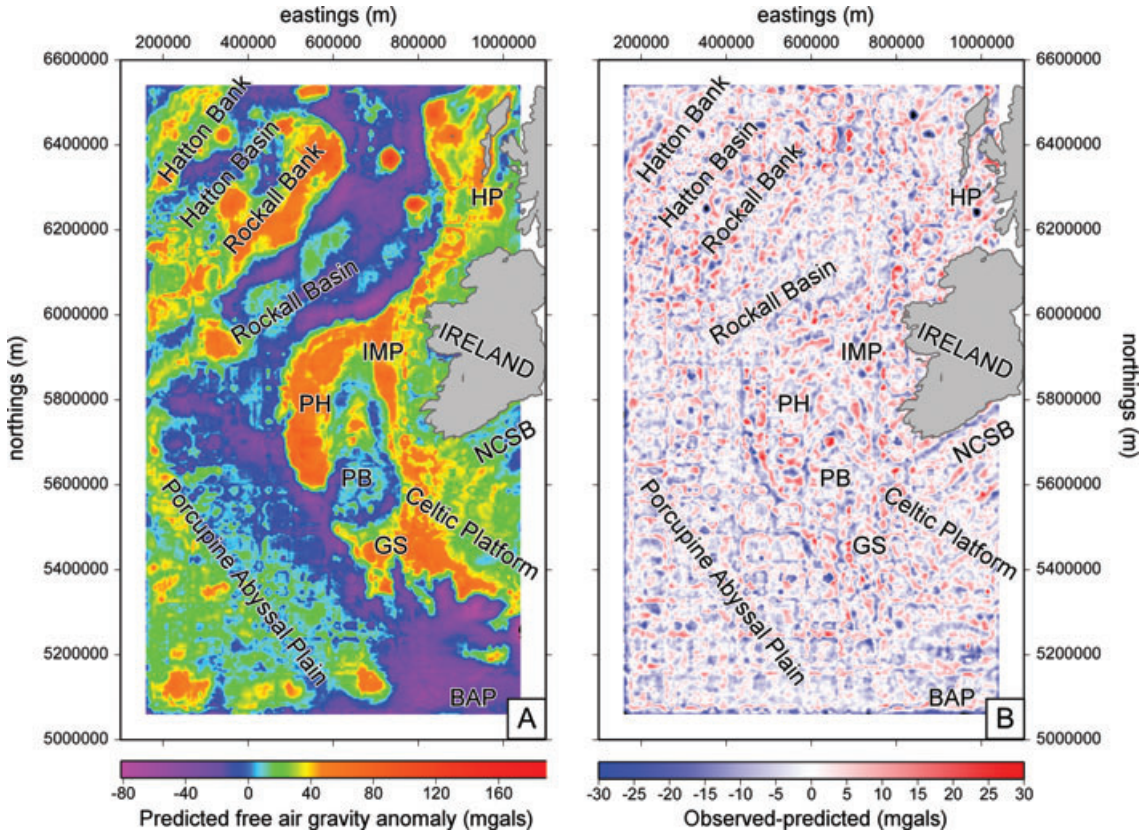

Figure 4. Predicted free air gravity anomaly map from the inverted density anomaly model (A) and the difference between these predicted data and the observed data shown in Fig. 2(D) (B). Key bathymetric structures of the margin are labelled in black on both plots. Bathymetric structure abbreviations as in the caption for Fig. 2.

and vertical striping is observed in the predicted data due to the parametrization used for the inversion but this does not detract from the broad results. The overall fit between the observed and predicted gravity anomalies can be assessed by examining their difference plot (Fig. 4B). This plot shows that the differences are all well below 30 mGals throughout the study region and that all areas show similar fits. Overall, the inversion managed to successfully reproduce all of the long wavelength data trends and most of the short wavelength anomalies.

5.4.1 Moho variations

The Moho discontinuity marks the seismic boundary between the crust and mantle. Below this boundary, which can be abrupt or gradational, seismic P-wave velocity is generally greater than 7.9 km s^{-1} for the Irish crust (Lowe & Jacob 1989; Hauser *et al.* 2008). Determining the location and structure of the Moho can be accomplished using wide-angle reflection/refraction profiling (WARRP). The Moho depth compilation from Kelly *et al.* (2007) obtained by interpolating between seismic refraction results over the Irish margin (and beyond) is shown in Fig. 5(A). Since the Moho is classically defined as a seismic discontinuity, it is not generally defined in terms of a specific density contrast. Nonetheless, an attempt to extract information about Moho structure from the density anomaly model can be made by defining a Moho-proxy that corresponds with the 170 kg m^{-3} isosurface (3020 kg m^{-3} relative to a reference density of 2850 kg m^{-3}). It should be stressed that by using this Moho-proxy, the assumption is made that Moho variations are the primary cause of subbasin mass variations rather than internal mass variations within the crust and/or mantle. Generally, an excellent agreement is observed in most places between the interpolated seismic Moho from Kelly *et al.* (2007) and the density anomaly Moho-proxy from this study. Where there is a disagreement, the cause can generally be explained by the lack of or poorer quality of nearby seismic constraints (Fig. 5C). Generally, an excellent correspondence is observed between the inverted Moho from this study and the depth to Moho derived in Kimbell *et al.* (2010).

Similar patterns of Moho deepening and shallowing are observed for both the interpolated Kelly *et al.* (2007) seismic results (Fig. 5A) and the gravity inversion results (Fig. 5B) although the magnitude of these fluctuations varies. While the match between the Moho depths for the Hatton Bank, Rockall Bank and Hebridean Platform is generally very good, Kelly *et al.* (2007) resolve a deeper Moho beneath the Porcupine High and the Irish Mainland Platform than does the gravity inversion despite the seismic constraints used for the Porcupine High in the compilation appearing shallower in their source publication (Whitmarsh *et al.* 1974). The deep Moho from Kelly *et al.* (2007) beneath the Irish Mainland Platform may also simply reflect the seaward extrapolation of Moho depths obtained from land seismic surveys (not shown on figure).

The greatest discrepancy in Moho depth (on the order of 8 km) between the seismic and gravity inversion results exists for the Goban Spur where Kelly *et al.* (2007) resolve a significantly deeper Moho. This extreme Moho deepening which lies immediately to the north of the Biscay Abyssal Plain, is constrained solely by the sparse seismic results from Ginzburg *et al.* (1985) which are very poorly constrained at the landward end of the profile. Meanwhile, Kimbell *et al.* (2010) also resolve a shallower Moho at comparable depth to the Moho from this study.

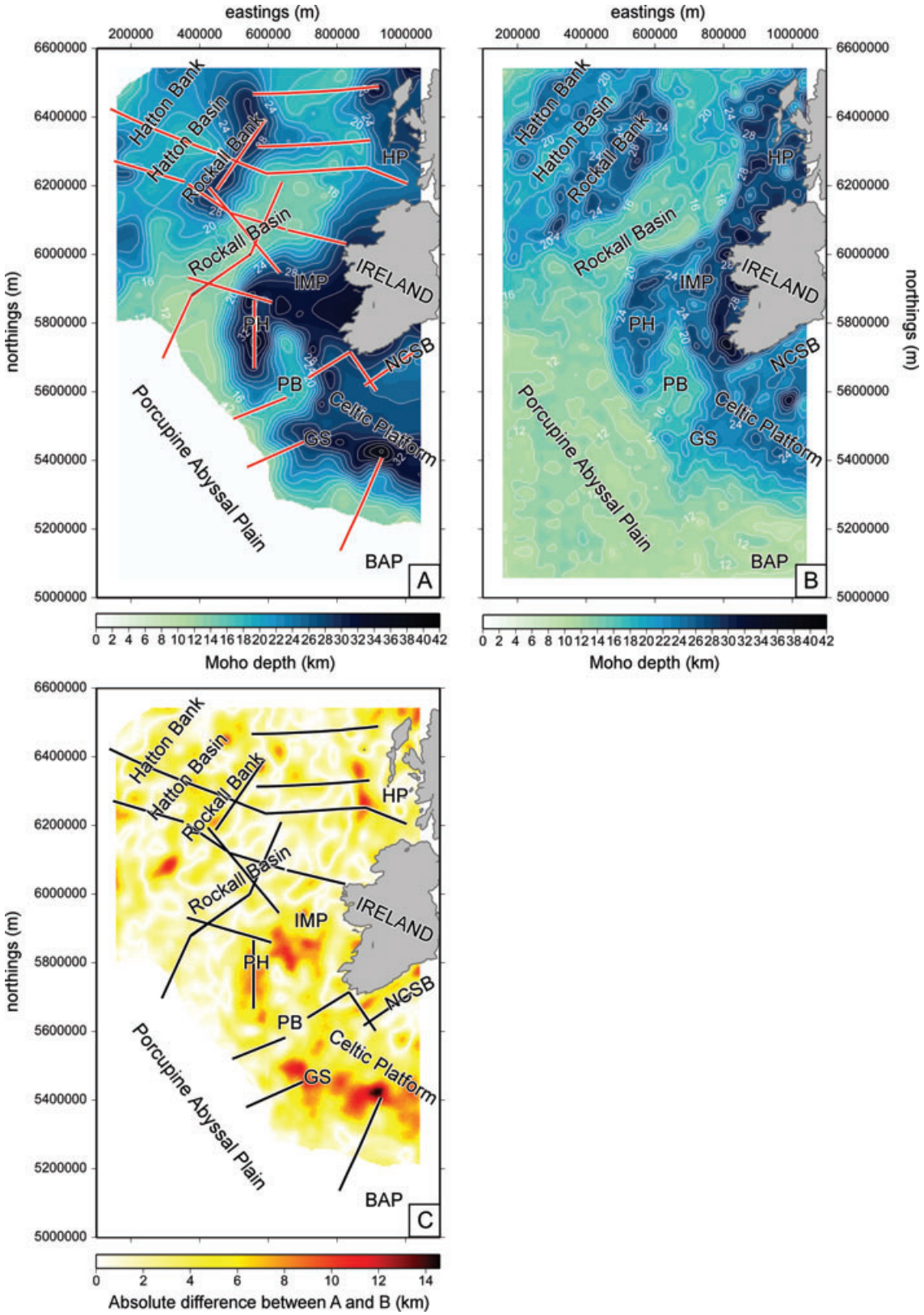

Figure 5. Maps of Moho depths, (A) from the seismic compilation from Kelly *et al.* (2007) with constraining seismic lines shown in red, and (B) from the 170 kg m^{-3} anomaly isosurface of the inverted density anomaly model. Plot (C) shows the absolute difference between plots (A) and (B). The constraining seismic profiles from Kelly *et al.* (2007) are also shown in plot (C). Key bathymetric structures of the margin are labelled in black on all plots. Bathymetric structure abbreviations as in the caption for Fig. 2.

The shallowing of the Moho beneath the Rockall and Porcupine basins is almost certainly due to stretched and thinned crust. Meanwhile, the complex transition between the southern Porcupine Basin and the Goban Spur corresponds to an area where there is a combination of (1) igneous centres, (2) structural basement highs and (3) caledonoid/variscide ENE–SWS structural fabrics.

Along the northeast trending axis of the Rockall Basin, the Moho from both the seismic compilation (Fig. 5A) and the gravity inversion (Fig. 5B) shows a gradual deepening from 12 km down to 18 km in the northeast with a number of short wavelength variations superimposed. The variations may correspond to different amounts of igneous intrusions, possibly related to the formation of oceanic crust (Scrutton 1986; Bentley & Scrutton 1987; Megson 1987), exhumed serpentinized mantle (O'Reilly *et al.* 1996) and/or different basement/crustal terranes. Beneath the Porcupine Abyssal Plain where few seismic constraints are available, the gravity inversion results yield a consistently flat Moho at approximately 12 km depth.

One interesting trend observed in the gravity inversion results is the sharp contrast in Moho character exhibited immediately to the south of the Irish mainland. The prominent southwest–northeast boundary separating these two zones may mark the northern limit of crustal decoupling that accommodated slight thinning beneath the Irish and Celtic Sea regions (O'Reilly *et al.* 1991) relative to the thicker crust to the north (Lowe & Jacob 1989; Hauser *et al.* 2008). This trend is also observed in the Moho structure from Kimbell *et al.* (2010) but is slightly less pronounced.

Fig. 6 shows a selection of slices through the inverted density anomaly model along two seismic profiles included in the Kelly *et al.* (2007) compilation, G3 and RAPIDS1 (Ginzburg *et al.* 1985; O'Reilly *et al.* 1995; Vogt *et al.* 1998), and three more recent seismic profiles not included in the compilation, BM05, R4 and W08 (Bullock & Minshull 2005; O'Reilly *et al.* 2006; White *et al.* 2008). Above each slice, the comparison between the corresponding observed (blue) and predicted (red) gravity anomalies is plotted. In general, these slices highlight the excellent correspondence between the Moho from the seismic interpolation and the gravity inversion. One key exception to this is for profile W08 where the Moho structure captured by the more recent seismic work more closely matches the gravity inverted Moho-proxy while the earlier Kelly *et al.* (2007) compilation underestimates the depth and structure of the Moho.

Another peculiar mismatch between the Kelly *et al.* (2007) compilation and the results from this study is observed at the western limit of profile R4 (O'Reilly *et al.* 2006). Here the Kelly *et al.* (2007) compilation shows a significant deepening of the Moho to 35 km depth beneath the Porcupine High while the original seismic survey over the Porcupine High by Whitmarsh *et al.* (1974) revealed a Moho depth of 28 km, closer to the Moho depth resolved from the gravity inversion.

One of the great advantages of generating a 3-D density anomaly model is that the model can be sliced to provide cross-sections across regions where no corresponding seismic lines exist. A number of such cross-sections are plotted as a fence diagram in Fig. 7. These slices highlight some of the discrepancies in Moho depths between the Kelly *et al.* (2007) compilation and the gravity inversion results from this study. Ignoring the possibly erroneous seismic constraints beneath the Porcupine High and the Goban Spur, the gravity inversion results demonstrate a distinct difference between these two blocks with the Goban Spur appearing to have undergone significantly more thinning and extension. This juxtaposition, which is also observed by Kimbell *et al.* (2010), is not surprising since the Goban Spur and the Celtic Platform both lie in the Variscan crustal domain and probably experienced a different amount of extension (particularly the complex Goban Spur which has structural features of both Variscan (ENE–WSW) and Atlantic (N–S) tectonism) and this may explain the thinner crust. Meanwhile, if the seismic constraints are reliable and the discrepancy is real, this would signify that the lower crust of the Goban Spur was of anomalously high density, possibly due to sill intrusion or an underplated body, such that the density anomaly chosen as the Moho-proxy was too low in this region. Further seismic surveying in the region is required to definitively resolve this discrepancy.

5.4.2 *Density variations in the crust*

Similar to the approach used in Welford & Hall (2007), the crust is subdivided into upper, middle and lower crust according to density anomaly values relative to 2850 $\mathrm{kg\,m^{-3}}$. These subdivisions, which are delineated by the dashed grey lines on the slices in Fig. 6, are intended to simplify description of the crustal density variations and aid in their interpretation. The upper crust is defined as corresponding to density anomaly values of less than $-80\ \mathrm{kg\,m^{-3}}$, middle crust as corresponding to density anomaly values between -80 and 20 $\mathrm{kg\,m^{-3}}$ and lower crust as corresponding to density anomaly values between 20 and 170 $\mathrm{kg\,m^{-3}}$.

Combining the depth to basement constraints (Fig. 2B) with the inverted Moho depth model (Fig. 5B), the resulting map of crustal basement thickness across the margin (Fig. 8A) can be used to analyse variations in the thickness of individual crustal layers. To highlight these variations further, the thickness of the upper, middle and lower crust are plotted as a percentage of the total crustal thickness in Figs 8(B)–(D), respectively.

Lower densities which have been categorized as upper crustal dominate up to 40 per cent of the crust within regions of continental crust in Fig. 8(B) while representing a much lower percentage in regions of extensively thinned continental crust, exhumed serpentinized mantle and oceanic crust. Thus, the 10 per cent contour in Fig. 8(B) highlights the edges of continental blocks such as the Hatton Bank, the Rockall Bank, the Hebridean Platform, the Porcupine High, the Irish Mainland Platform, the Goban Spur and the Celtic Platform.

From the map of the percentage of middle crustal densities (Fig. 8C), several trends are observed. Middle crustal densities occupy about 30 per cent of the 'classic' oceanic crust of the Porcupine Abyssal Plain and of the continental blocks highlighted by similar percentages of upper crustal densities. Meanwhile, the Goban Spur is characterized by a slightly higher percentage of middle crustal densities as is the northwest margin of the Rockall Basin and the edges of the Porcupine basin. For the edges of the extensional basins, this focusing of higher density material may be caused by outward-directed lower crustal flow induced from erosion of the rift flanks which increases the vertical loading in the centre of the basins as modelled by Burov & Cloetingh (1997).

The most startling revelation from the mapping of crustal layer thickness percentages can be observed in Fig. 8(D) where lower crustal densities dominate over 50 per cent of the crust within the Porcupine Basin, the Rockall Basin, outboard of the Porcupine High and Goban Spur and south of the Celtic Platform. In all of these regions, other than south of the Celtic Platform, these dominant lower crustal densities correspond with occurrences of exhumed serpentinized mantle which have been interpreted from previous seismic studies (O'Reilly *et al.* 1996; Reston *et al.* 2001, 2004;

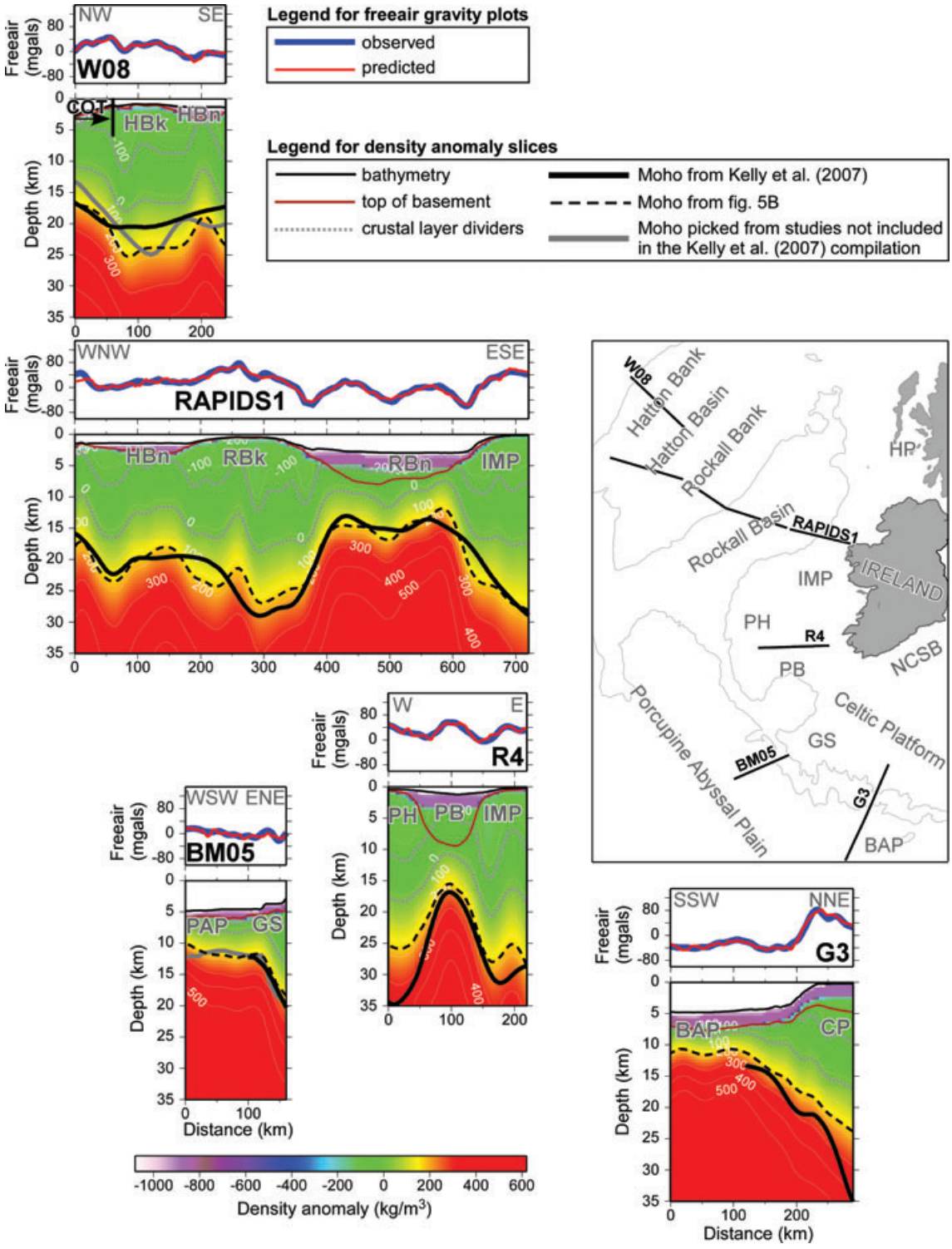

Figure 6. Slices through the inverted density anomaly model along selected seismic lines of the study region. A comparison between the observed free air gravity anomalies (blue line) and the anomalies predicted for the inverted density anomaly model (red line) is plotted above each slice. The overlain thick black lines on the density anomaly slices correspond to the Moho depths obtained from the compilation from Kelly *et al.* (2007) and the dashed black lines are from this study. The thick grey lines are from more recent seismic studies not included in the Kelly *et al.* (2007) compilation. The dashed gray lines separate inferred upper, middle and lower crustal layers. Labelled line locations are plotted on the simplified bathymetry map. Key bathymetric features of the margin are labelled on the slices and on the map. Bathymetric structure and other abbreviations: BAP, Biscay Abyssal Plain; COT, continent–ocean transition; GS, Goban Spur; HBk, Hatton Bank; HBn, Hatton Basin; HP, Hebridean Platform; IMP, Irish Mainland Platform; NCSB, North Celtic Sea Basin; PAP, Porcupine Abyssal Plain; PB, Porcupine Basin; PH, Porcupine High; RBk, Rockall Bank; RBn, Rockall Basin.

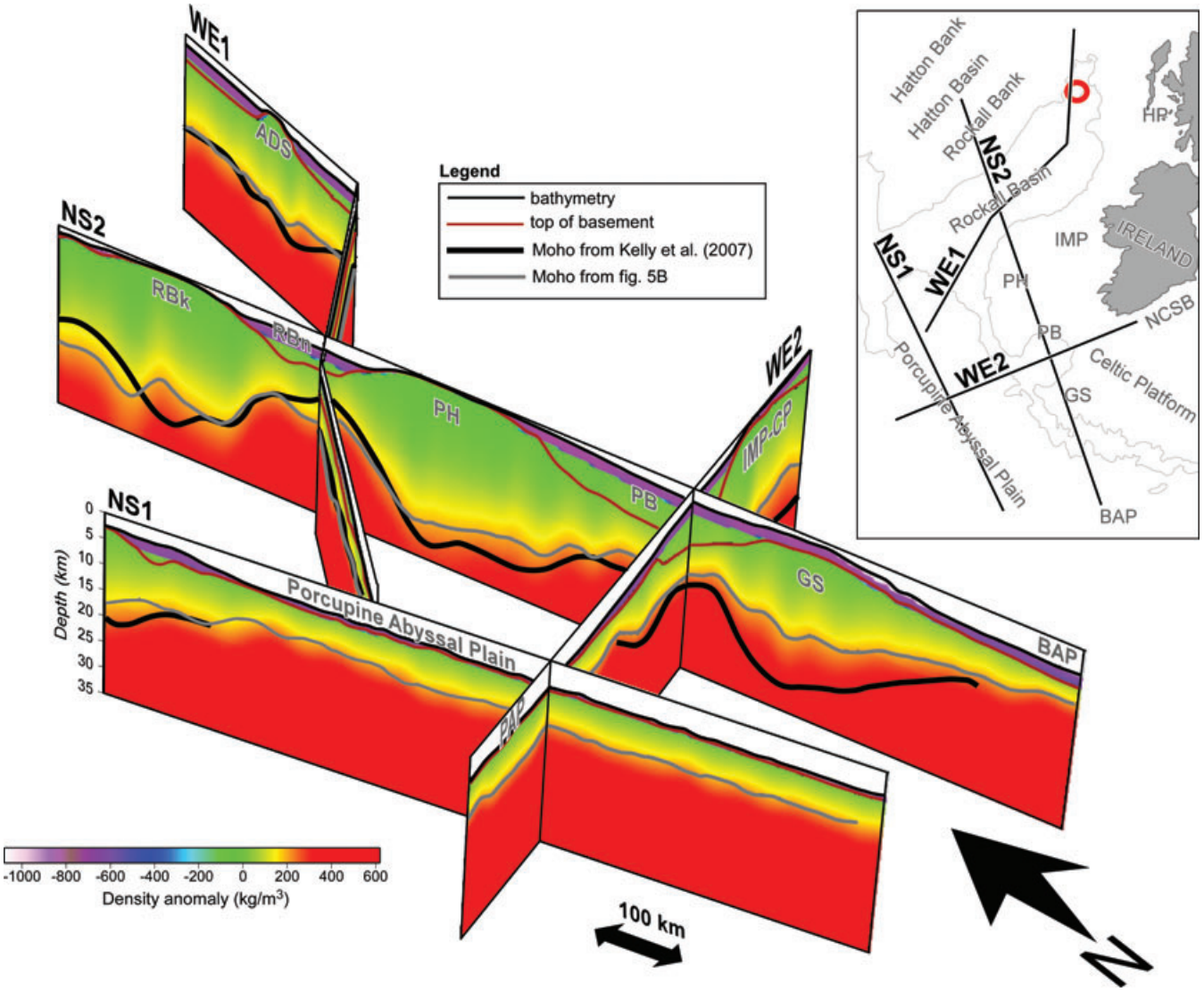

Figure 7. Fence diagram of arbitrary slices through the inverted density anomaly model with the slice locations plotted on the simplified bathymetry map. The overlain thick grey lines on the density anomaly slices correspond to the Moho depths obtained from this study (Fig. 5B) and the thick solid black lines correspond to the Moho depths from the Kelly *et al.* (2007) interpolation. On the map, the location of the Anton Dohrn Seamount is shown by the red circle. Key bathymetric features of the margin are labelled on the slices and on the map. Bathymetric structure abbreviations as in caption for Fig. 6.

Bullock & Minshull 2005; O'Reilly *et al.* 2006). It is not clear whether this relationship holds true for the region south of the Celtic Platform based on the vintage seismic results from Ginzburg *et al.* (1985) but further seismic investigation is warranted. If the zones dominated by lower crustal densities are representative of zones of exhumed serpentinized mantle, mapping these regions provides a tool for predicting zones of exhumed serpentinized mantle in regions lacking seismic coverage.

6 DISCUSSION

The 3-D density anomaly model derived from the gravity inversion provides an independent view of the Irish Atlantic continental margin that complements existing seismic data sets and provides further insight into the structure of the margin. Combining the depth to basement constraints (Fig. 2B) with the inverted Moho depth model (Fig. 5B), the resulting map of crustal basement thickness across the margin (Fig. 8A) can be used to analyse variations in crustal extension or compared against overlying sediment thicknesses to search for evidence of faults and detachments. It should be highlighted that the crustal basement thickness derived from this study is very similar to that derived by Kimbell *et al.* (2010) while requiring far less *a priori* information for the generation of the equivalent model. Consequently, constrained regional gravity inversion as performed in this study provides a robust tool that can be used in lightly explored regions to obtain detailed crustal knowledge.

6.1 Variations in crustal extension

Variations in the amount of extension experienced over a given margin can reveal trends in the variations in rifting style. Such variations are often investigated by computing the cumulative offset and

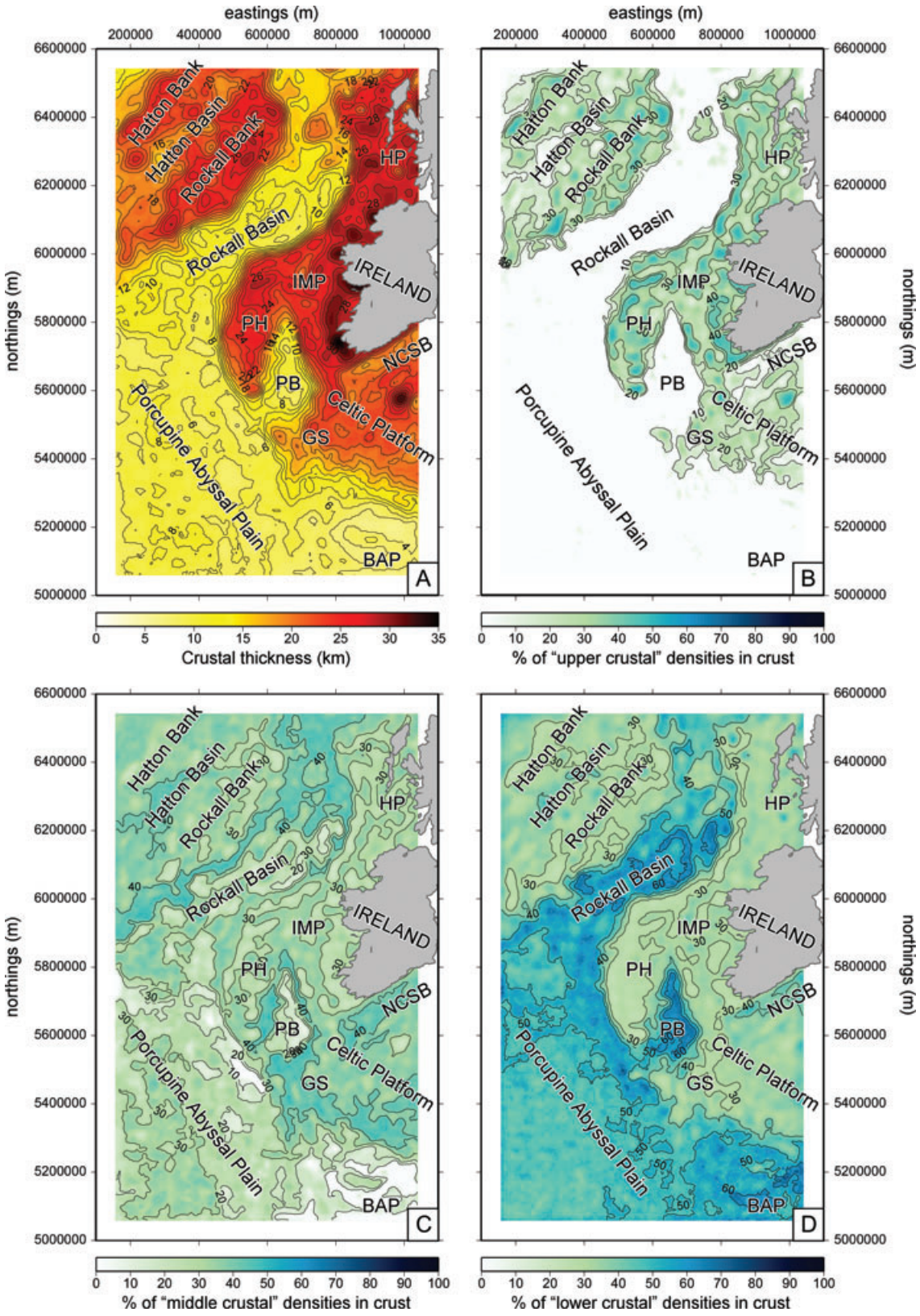

Figure 8. Maps of (A) crustal basement thickness computed from depth to basement (Fig. 2B) and the interpreted Moho depth surface (Fig. 5B), (B) percentage of the total crustal basement thickness with density anomalies below –80 kg m^{-3} (i.e. upper crustal type densities), (C) percentage of the total crustal basement thickness with density anomalies between −80 and 20 kg m^{-3} (i.e. middle crustal type densities) and (D) percentage of the total crustal basement thickness with density anomalies between 20 and 170 kg m^{-3} (i.e. lower crustal type densities). Key bathymetric structures of the margin are labelled in black on all plots. Bathymetric structure abbreviations as in caption for Fig. 2.

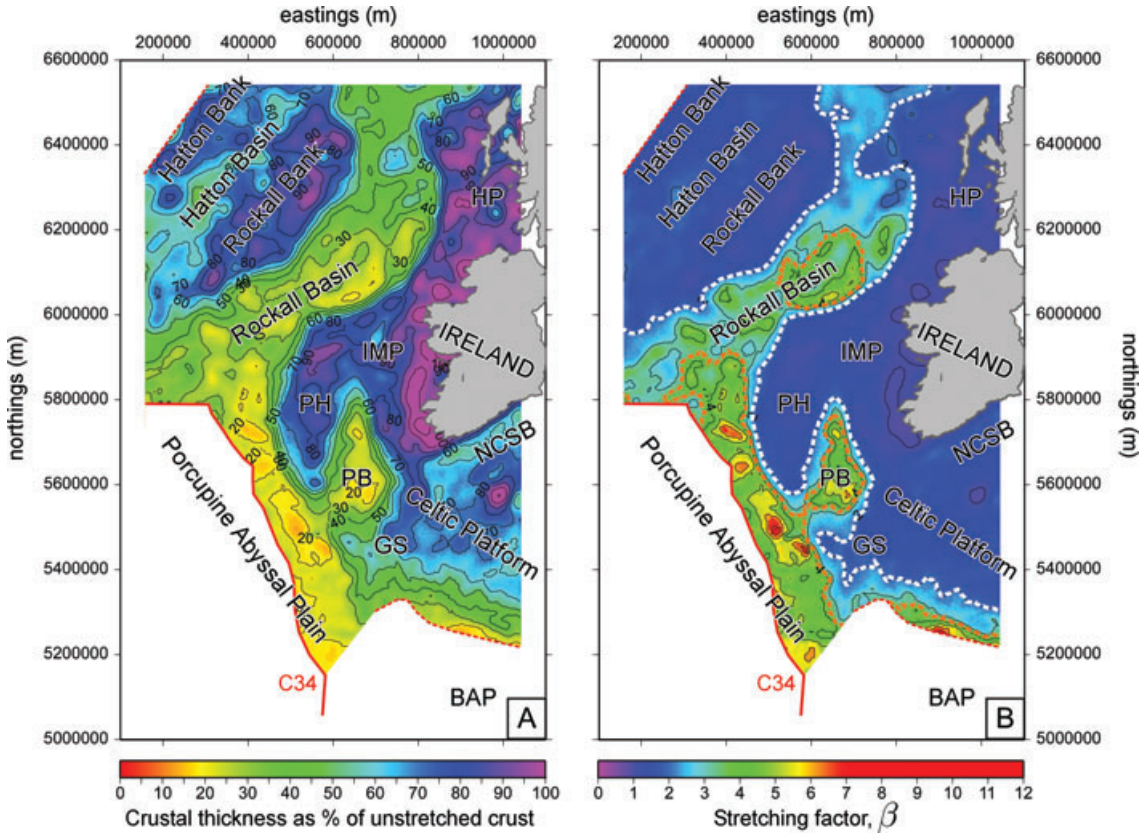

Figure 9. Maps of project area showing (A) crustal thickness as a percentage of the unstretched thickness of the Irish Atlantic margin (30 km; Lowe & Jacob 1989; Hauser *et al.* 2008) and (B) stretching factor, β. Regions corresponding to oceanic crust from Müller *et al.* (2008) outboard of Hatton Bank and into the Bay of Biscay have been masked out of both maps (limit shown by dashed red line). Outboard of the main study area, magnetic anomaly C34 (solid red line; Srivastava *et al.* (1988a)) is used to define the onset of normal seafloor spreading since exhumed serpentinized mantle has been interpreted inboard of this boundary (Bullock & Minshull 2005). On both plots, the $\beta = 2$ contour, corresponding to the stretching factor above which polyphase faulting becomes important (Reston 2007), and the $\beta = 3.5$ contour, corresponding to the stretching factor above which embrittlement of the entire crust is possible (Pérez-Gussinyé. & Reston 2001; Pérez-Gussinyé *et al.* 2003), are highlighted by the white and orange dotted lines, respectively. Bathymetric structure abbreviations as in caption for Fig. 2.

displacement across well imaged faults on good quality seismic reflection data. Alternatively, crustal-scale models derived from seismic refraction or other geophysical techniques can be used (e.g. Reston 2007). For this study, extension across the Irish Atlantic continental margin is investigated directly using the gravity inversion results.

Crustal thickness, plotted as a percentage of the unstretched thickness of the Irish Atlantic margin (30 km; Lowe & Jacob 1989; Hauser *et al.* 2008), is shown in Fig. 9(A). Estimates of the extension/stretching factor, β, across the margin are computed on the basis of the computed crustal thickness and are shown in Fig. 9(B). The extension factor, which corresponds to the ratio of extended length to unextended length, was computed by taking a 1-km-long block of 30-km-thick crust and computing the extended length for the varying crustal thicknesses in the study region by assuming that the cross-sectional area remains constant.

Crustal thickness across the Irish Atlantic continental margin shows relatively predictable trends with the thickest crust surrounding the Irish mainland, slightly thinner crust beneath the rifted Rockall and Hatton banks and finally the thinnest crust beneath the major sedimentary depocentres such as the Rockall and the Porcupine basins. As previously mentioned, the thinner crust of the Goban Spur and Celtic Platform relative to the Irish Mainland Platform and the Porcupine High are due to the former lying in the Variscan crustal domain and likely experiencing a different amount of extension.

Examination of the computed stretching factors reveals more interesting and less predictable details of the margin (Fig. 9B). To aid in highlighting the key observations, two key contours are enhanced. The first, where $\beta = 2$ and indicated by the dotted white line, corresponds to the stretching factor above which polyphase faulting becomes important and older faulting can be obscured by younger faulting making it difficult to quantify the total amount of extension based on seismically imaged faults alone (Reston 2007). Based on this contour, it would appear that the amount of extension experienced by most of the moderately stretched Irish Atlantic continental margin can be accurately assessed using available seismic reflection data.

The second highlighted contour in Fig. 9(B), where $\beta = 3.5$ and indicated by the dotted orange line, corresponds to the stretching factor above which embrittlement of the entire crust is thought to be possible based on numerical modelling studies (Pérez-Gussinyé & Reston 2001; Pérez-Gussinyé *et al.* 2003). Total crustal embrittlement can result in the serpentinization of the upper mantle along faults that cross-cut the entire crust. Based on this contour, zones of mantle serpentinization would be expected beneath the Porcupine Basin, within pockets beneath the Rockall Basin and outboard of both the Porcupine High and the Goban Spur. For the

Rockall Basin, the Porcupine Basin and outboard of the Goban Spur, these zones may correspond with zones of exhumed serpentinized mantle interpreted on the basis of anomalously low upper mantle velocities from previous seismic refraction studies (O'Reilly *et al.* 1996; Reston *et al.* 2001, 2004; Bullock & Minshull 2005; O'Reilly *et al.* 2006).

6.2 Sediment excess and deficiency on the margin

As a conceptual tool for assessing sediment excess and deficiency on the Irish Atlantic continental margin, comparisons can be made between the inferred crustal thickness (Fig. 8A) and the observed sediment thickness (Fig. 2C). For this exercise and for simplicity, local isostasy is assumed. While Daly *et al.* (2004) have resolved northwestward variations in the effective elastic thickness of the lithosphere from the Irish Mainland Platform across the Rockall and Hatton banks which follow the NE–SW trend of the Caledonian front, the effective elastic thickness of the lithosphere of the entire Irish Atlantic margin generally appears to be quite low regardless of the method used to derive it (Warner 1987; Kusznir *et al.* 1995; Chadwick & Pharaoh 1998). Consequently, local isostatic balance is a valid first-order approximation over the geographic scale of interest and regardless of the exact mechanism of compensation.

Assuming local Airy compensation and constant densities for water (ρ_w), sediments (ρ_s), crust (ρ_c) and mantle (ρ_m), then sediment thickness (s) is inversely proportional to the amount of crustal thinning (dt) below the sediments such that

$$s = \mathrm{d}t(\rho_m - \rho_c)/(\rho_m - \rho_s) - W(\rho_m - \rho_w)/(\rho_m - \rho_s). \quad (1)$$

Using water depth (W) obtained from the bathymetry and assuming that the crust was 30 km thick before thinning (Lowe & Jacob 1989), and that ρ_w , ρ_s, ρ_c and ρ_m are 1030, 2200, 2850 and 3300 kg m^{-3}, respectively, deviations from the model of isostatically compensated sediment thickness for a given crustal thickness are shown in Fig. 10 where areas of sediment deficiency correspond to blue and those of excess correspond to red. The choice of sediment density results in modest overcompensation in deep water, but the value of the approach is in the ability to identify strong gradient zones as was done in Welford & Hall (2007).

Overlain on Fig. 10 are the main bounding faults of the sedimentary basins on the Irish margin (indicated in green). Since initial location and orientation of the Irish offshore basins is thought to have been influenced largely by pre-existing structural fabrics and major basement structures of Variscan, Caledonian and older orogenic age (Shannon 1991; Naylor & Shannon 2009), it is not surprising that many of the trends in the sediment difference map follow the trends associated with those structural fabrics. While most of the strong gradients in the sediment difference map arguably have NW-SE trends which are perpendicular to and which highlight faults with a NE–SW Caledonian orientation, individual basins often exhibit more than one trend.

The margins of the Rockall Basin generally correspond with strong gradients in the sediment difference plot (Fig. 10) and the basin itself contains pockets of excess sediments along most of its length. These excess sediments are consistent with an episode of increased sedimentation during the Cenozoic (Stoker 1997) that has been attributed to an anomalously high rate of subsidence at that time (Clift & Turner 1998). The increased rate of subsidence observed from borehole stratigraphy and high resolution seismic reflection data may have resulted from the temporal evolution of post-rift small-scale upper mantle convective currents (Praeg *et al.* 2005).

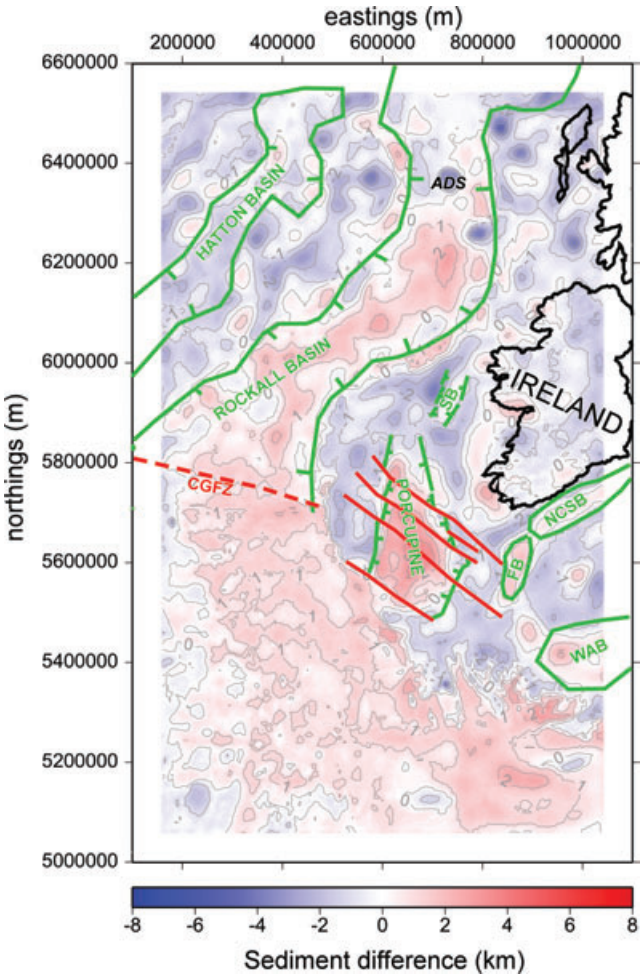

Figure 10. Sediment thickness difference map with the main basin-bounding faults shown as green lines and basin names labelled in green. Dominant northwest–southeast faults within the Porcupine Basin are plotted as solid red lines and the Charlie-Gibbs Fracture Zone (CGFZ) is plotted as the dashed red line. Abbreviations: ADS, Anton Dohrn Seamount; FB, Fastnet Basin; NCSB, North Celtic Sea Basin; SB, Slyne Basin; WAB, Western Approaches Basin.

The processes of enhanced subsidence and sedimentation in the Rockall Basin are also responsible for the pronounced sediment excess observed for the Porcupine Basin (Fig. 10). In fact, due to the greater amount of extension experienced by the Porcupine Basin and how much closer it came to complete crustal separation, local upper mantle convective flow may have enhanced subsidence in this area relative to the Rockall Basin, resulting in the greater amount of sediment excess. Strong gradients oriented east-west and southwest-northeast mark the edges of the Porcupine Basin with the steeper gradient on its western margin consistent with results from other studies (O'Reilly *et al.* 2006; Kimbell *et al.* 2010). To the south of the Porcupine Basin, both the northern and southern edges of the Goban Spur, which itself contains several sedimentary half-graben basins, are also characterized by sediment difference gradients (Fig. 10). These gradients which are perpendicular to and which delineate faults that are aligned with the continent-ocean boundary, are likely associated with east-west extension and opening of the North Atlantic Ocean.

The Slyne Basin on the Irish Mainland Platform shows neither a sediment deficit or excess although its northwest border is marked by a localized zone of sediment deficit. Sediment isostatic equilibrium in the Slyne Basin may be partly due to the fact that it is a small basin that tended to be filled to capacity partly by being close to sediment provenance areas, by having a number of inversion episodes that uplifted the region and also by the fact that it is a basin overlying a region of relatively low crustal stretching so that its thermal and subsidence behaviour is different from the large high-extension basins such as Porcupine and Rockall.

South of the Irish mainland, the ENE–WSW trending North Celtic Sea Basin is characterized by a moderate sediment excess despite having experienced both Alpine inversion and low sedimentation during Cenozoic times. This may be explained by a combination of an initially thicker crust in late Variscan times and hence the development of intermontane Permo-Triassic clastic depocentres (Štolfovà. & Shannon 2009). A similar explanation is suggested for the apparent moderate sediment excess for the Western Approaches Basin on the continental shelf of the Celtic Platform.

At the northwestern limit of the study area, two thirds of the southwestern portion of the Hatton Basin, a Mesozoic failed rift, are characterized by a sediment deficit. This deficit can be attributed to an episode of thermal uplift following the intrusion of hot mantle material into the lower crust (White & McKenzie 1989; Makris *et al.* 1991).

The NNE–SSW trending Fastnet Basin is characterized by a moderate sediment excess which can be attributed to an igneous contribution from a localized hotspot (Caston *et al.* 1981; Shannon 1995). The crustal thickness inferred from the inversion is thinner than would be expected given the extra crustal thickening due to intrusions giving the impression that there is a sediment excess.

Overall, the sediment difference map (Fig. 10) appears to highlight inherited Caledonian basement structures and fabrics for most areas of the margin. Meanwhile, areas where pre-existing Caledonian and Variscan trends are not apparent may represent zones where the deformation from those orogenies was less pronounced or where zones of anomalous crust exist. Ultimately, the unique view of the Irish continental margin provided by the study may prove useful for future more detailed palaeoreconstructions of the North Atlantic region prior to rifting.

7 CONCLUSIONS

A constrained 3-D gravity inversion of the free air data over the Irish Atlantic continental margin was undertaken and a regional density anomaly model was generated that is in agreement with constraints obtained from seismic and other methods. An independent proxy for Moho structure was obtained by defining a density anomaly isosurface and this information was combined with available sediment thickness estimates to enable the investigation of variations in upper, middle, lower and total crustal thickness as well as variations in the degree of extension across the margin. Key findings include:

(i) The Moho proxy obtained from the regional gravity inversion in this study agrees (within less than 5 km) with over 80 per cent of the Moho constraints obtained from a recent compilation of seismic refraction results over the Irish margin. The inverted Moho is also in excellent agreement with the Moho structure obtained from a more recent study involving combined regional forward gravity modelling and targeted gravity inversion of key lithospheric layers while the results obtained from the present study required far less a priori information and regularization.

(ii) Regions where the crust is dominated by lower crustal densities appear to correspond with zones of exhumed serpentinized mantle as interpreted from seismic refraction modelling. The areal mapping of these crustal zones, which also stand out from maps of estimated extension factors, may allow for the extrapolation of zones of exhumed mantle into regions lacking seismic coverage.

(iii) Assuming local isostatic compensation for simplicity, where sediment thicknesses deviate from those expected for a compensated crust, trends generally highlight inherited Caledonian basement structures and fabrics.

In all, the inversion results provide a unique perspective of the Irish Atlantic continental margin that complements results from previous seismic and geophysical studies. Insights gleaned from the findings may provide further constraints for future palaeoreconstructions of North Atlantic rifting and may direct the focus of future geophysical investigations.

ACKNOWLEDGMENTS

The collaboration for this study evolved from a North Atlantic Petroleum Systems Assessment (NAPSA) Workshop that took place in St. John's, NL, Canada in July of 2007. We thank the Irish Newfoundland Partnership for providing travel support which enabled further discussions in Dublin, Ireland in July of 2009. We would like to thank the Natural Sciences and Engineering Research Council of Canada for postdoctoral funding for Welford and for a Discovery Grant to Hall.

REFERENCES

Albertz, M., Beaumont, C., Shimeld, J., Ings, S. & Gradmann, S., 2010. An investigation of salt tectonic structural styles in the Scotia Basin, offshore Atlantic Canada: 1. Comparison of observations with geometrically simple numerical models, *Tectonics*, **29**, TC4017, doi:10.1029/2009TC002539.

Andersen, O., Knudsen, P., Berry, P., Freeman, J., Pavlis, N. & Kenyon, S., 2008. The DNSC08 ocean wide altimetry derived gravity field, in *EGU 2008 Meeting Programme,* Abstract EGU2008-A-07163; G1-1MO1O-003.

Athy, L., 1930. Density, porosity, and compaction of sedimentary rocks, *AAPG Bull.,* **14**(1), 1–24.

Bentley, P. & Scrutton, R., 1987. Seismic investigations into the basement structure of southern Rockall Trough, in *Petroleum Geology of North West Europe: Proceedings of the Third Conference,* pp. 667–675, eds Brooks, J. & Glennie, K., Graham and Trotman, London.

Bullock, A.D. & Minshull, T.A., 2005. From continental extension to seafloor spreading: crustal structure of the Goban Spur rifted margin, southwest of the UK, *Geophys. J. Int.,* **163,** 527–546.

Burov, E. & Cloetingh, S., 1997. Erosion and rift dynamics: new thermomechanical aspects of post-rift evolution of extensional basins, *Earth planet. Sci. Lett.,* **150,** 7–26.

Caston, V., Dearnley, R., Harrison, R., Rundle, C. & Style, M., 1981. Olivine-dolerite intrusions in the Fastnet Basin, *J. geol. Soc. Lond.,* **138,** 31–46.

Chadwick, R. & Pharaoh, T., 1998. The seismic reflection Moho beneath the United Kingdom and adjacent areas, *Tectonophysics,* **299,** 255–279.

Clift, P. & Turner, J., 1998. Paleogene igneous underplating and subsidence anomalies in the Rockall-Faeroe-Shetland area, *Mar. Petrol. Geol.,* **15,** 223–243.

Daly, E., Brown, C., Stark, C. & Ebinger, C., 2004. Wavelet and multitaper coherence methods for assessing the elastic thickness of the Irish Atlantic margin, *Geophys. J. Int.,* **159,** 445–459.

de Graciansky, P. & Poag, C., 1985. Geologic history of Goban Spur, northwest Europe continental margin, in *Initial Reports of the DSDP,* Vol. 80,

Chap. 58, pp. 1187–1216, eds de Graciansky, P. & Poag, C., US Government Printing Office, Washington, DC.

de Graciansky, P., Poag, C. & Foss, G., 1985. Drilling on the Goban Spur: objectives, regional geological setting, and operational summary, in *Initial Reports of the DSDP,* Vol. 80, pp. 5–13, US Government Printing Office.

Doré, A., Lundin, E., Jensen, L., Birkeland, O., Eliassen, P. & Fichler, C., 1999. Principal tectonic events in the evolution of the Northwest European Atlantic margin, in *Petroleum Geology of North West Europe: Proceedings of the Fifth Conference,* **Vol. 5,** pp. 41–61, eds Fleet, A. & Boldy, S., Geological Society.

Ginzburg, A., Whitmarsh, R., Roberts, D., Montadert, L., Camus, A. & Avedik, F., 1985. The deep seismic structure of the northern continental margin of the Bay of Biscay, *Ann. Geophys.,* **3**(4), 499–510.

Hall, J., Marillier, F. & Dehler, S.A., 1998. Geophysical studies of the structure of the Appalachian orogen in the Atlantic borderlands of Canada, *Canadian Journal of Earth Sciences,* **35**(11), 1205–1221.

Haughton, P., Praeg, D., Shannon, P., Harrington, G., Higgs, K., Amy, L., Tyrrell, S. & Morrissey, T., 2005. First results from shallow stratigraphic boreholes on the eastern flank of the Rockall Basin, offshore western Ireland, in *Petroleum Geology of North West Europe and Global Perspectives: Proceedings of the Sixth Petroleum Geology Conference,* pp. 1077–1094, eds Doré, A. & Vining, B., Geological Society of London.

Hauser, F., O'Reilly, B.M., Jacob, A.B., Shannon, P.M., Makris, J. & Vogt, U., 1995. The crustal structure of the Rockall Trough: differential stretching without underplating, *J. geophys. Res.,* **100**(B3), 4097–4116.

Hauser, F., O'Reilly, B., Readman, P., Daly, J. & van den Berg, R., 2008. Constraints on crustal structure and composition within a continental suture zone in the Irish Caledonides from shear wave wide-angle reflection data and lower crustal xenoliths, *Geophys. J. Int.,* **175,** 1254–1272.

Haworth, R. & Keen, C.E., 1979. The Canadian Atlantic margin: a passive continental margin encompassing an active past, *Tectonophysics,* **59,** 83–126.

Hitchen, K., Morton, A., Mearns, E., Whitehouse, M. & Stoker, M., 1997. Geological implications from geochemical and isotopic studies of Upper Cretaceous and Lower Tertiary igneous rocks around the northern Rockall Trough, *J. geol. Soc. Lond.,* **154,** 517–521.

Hopper, J., Funck, T., Tucholke, B., Louden, K., Holbrook, W. & Larsen, H.C., 2006. A deep seismic investigation of the Flemish Cap margin: implications for the origin of deep reflectivity and evidence for asymmetric break-up between Newfoundland and Iberia, *Geophys. J. Int.,* **164**(3), 501–515.

Jackson, M. & Talbot, C., 1986. External shapes, strain rates, and dynamics of salt structures, *Bull. geol. Soc. Am.,* **97**(3), 305–323.

Kelly, A., England, R.W. & Maguire, P.K., 2007. A crustal seismic velocity model for the UK, Ireland and surrounding seas, *Geophys. J. Int.,* **171,** 1172–1184.

Kimbell, G., Ritchie, J. & Henderson, A., 2010. Three-dimensional gravity and magnetic modelling of the Irish sector of the NE Atlantic margin, *Tectonophysics,* **486,** 36–54.

King, L., Fader, G., Poole, W. & Wanless, R., 1985. Geological setting and age of the Flemish Cap granodiorite, east of the Grand Banks of Newfoundland, *Can. J. Earth Sci.,* **22,** 1286–1298.

Kusznir, N., Roberts, A. & Morley, C., 1995. Forward and reverse modelling of rift basin formation, in *Hydrocarbon Habitat in Rift Basins,* Vol. 80, pp. 33–56, ed. Labiase, J., Geological Society of London, Special Publications.

Landes, M., Ritter, J., Readman, P. & O'Reilly, B., 2005. A review of the Irish crustal structure and signatures from the Caledonian and Variscan Orogenies, *Terra Nova,* **17**(2), 111–120.

Li, Y. & Oldenburg, D.W., 1996. 3-D inversion of magnetic data, *Geophysics,* **61**(2), 394–408.

Li, Y. & Oldenburg, D.W., 1998. 3-D inversion of gravity data, *Geophysics,* **63,** 109–119.

Lilly, H., 1965. Submarine examination of the Virgin Rocks area, Grand Banks, Newfoundland: preliminary note., *Geol. Soc. Am. Bull.,* **76**(1), 131–132.

Lowe, C. & Jacob, A.B., 1989. A north-south seismic profile across the Caledonian Suture zone in Ireland, *Tectonophysics,* **168,** 297–318.

Makris, J., Egloff, R., Jacob, A.B., Mohr, P., Murphy, T. & Ryan, P., 1988. Continental crust under the southern Porcupine Seabight, West of Ireland, *Earth planet. Sci. Lett.,* **89,** 387–397.

Makris, J., Ginzburg, A., Shannon, P., Jacob, A.B., Bean, C. & Vogt, U., 1991. A new look at the Rockall region, offshore Ireland, *Mar. Petrol. Geol.,* **8**(4), 410–416.

Megson, J., 1987. The evolution of the Rockall Trough and implications for the Faeroe-Shetland Trough, in *Petroleum Geology of North West Europe: Proceedings of the Third Conference,* pp. 653–665, eds Brooks, J. & Glennie, K., Graham and Trotman, London.

Morewood, N., Mackenzie, G., Shannon, P., O'Reilly, B., Readman, P. & Makris, J., 2005. The crustal structure and regional development of the Irish Atlantic margin, in *Petroleum Geology of North West Europe and Global Perspectives: Proceedings of the Sixth Petroleum Geology Conference,* pp. 1023–1033, eds Doré, A. & Vining, B., Geological Society of London.

Müller, R., Sdrolias, M., Gaina, C. & Roest, W., 2008. Age, spreading rates, and spreading asymmetry of the World's ocean crust, *Geochem., Geophys., Geosyst.,* **9**(Q04006), doi:10.1029/2007GC001743.

Naylor, D. & Shannon, P., 2005. The structural framework of the Irish Atlantic Margin, in *Petroleum Geology of North West Europe and Global Perspectives: Proceedings of the Sixth Petroleum Geology Conference,* pp. 1009–1021, eds Doré, A. & Vining, B., Geological Society, London.

Naylor, D. & Shannon, P., 2009. Geology of offshore Ireland, in *The Geology of Ireland,* 2nd edn, Chap. 17, pp. 405–460, eds Holland, C.H. & Sanders, I.S., Dunedin Academic Press, Edinburgh, UK.

Naylor, D., Shannon, P. & Murphy, N., 2002. Porcupine—Goban region—a standard structural nomenclature system, Special Publication 1/02, Petroleum Affairs Division, Dublin.

O'Reilly, B., Shannon, P. & Vogt, U., 1991. Seismic studies in the North Celtic Sea Basin - implications for basin development, *J. geol. Soc. Lond.,* **148,** 191–195.

O'Reilly, B.M., Hauser, F., Jacob, A.B., Shannon, P.M., Makris, J. & Vogt, U., 1995. The transition between the Erris and the Rockall basins: new evidence from wide-angle seismic data, *Tectonophysics,* **241,** 143–163.

O'Reilly, B.M., Hauser, F., Jacob, A.B. & Shannon, P.M., 1996. The lithosphere below the Rockall Trough: wide-angle seismic evidence for extensive serpentinisation, *Tectonophysics,* **255,** 1–23.

O'Reilly, B.M., Hauser, F., Ravaut, C., Shannon, P.M. & Readman, P., 2006. Crustal thinning, mantle exhumation and serpentinization in the Porcupine Basin, offshore Ireland: evidence from wide-angle seismic data, *J. geol. Soc. Lond.,* **163,** 775–787.

Pérez-Gussinyé, M. & Reston, T., 2001. Rheological evolution during extension at nonvolcanic rifted margins: onset of serpentinization and development of detachments leading to continental breakup, *J. geophys. Res.,* **106**(B3), 3961–3975.

Pérez-Gussinyé, M., Ranero, C., Reston, T. & Sawyer, D., 2003. Mechanisms of extension at nonvolcanic margins: evidence from the Galicia interior basin, west of Iberia, *J. geophys. Res.,* **108**(B5), doi:10.1029/2001JB000901.

Praeg, D., Stoker, M.S., Shannon, P., Ceramicola, S., Hjelstuen, B.O., Laberg, J.S. & Mathiesen, M., 2005. Episodic Cenozoic tectonism and the development of the NW European 'passive' continental margin, *Mar. Petrol. Geol.,* **22**(9-10), 1007–1030.

Reston, T., 2007. Extension discrepancy of North Atlantic nonvolcanic rifted margin: depth-dependent stretching or unrecognized faulting? *Geology,* **35**(4), 367–370.

Reston, T., Pennell, J., Stubenrauch, A., Walker, I. & Pérez-Gussinyé, M., 2001. Detachment faulting, mantle serpentinization, and serpentinite-mud volcanism beneath the Porcupine Basin, southwest of Ireland, *Geology,* **29**(7), 587–590.

Reston, T., Gaw, V., Pennell, J., Klaeschen, D., Stubenrauch, A. & Walker, I., 2004. Extreme crustal thinning in the south Porcupine Basin and the nature of the Porcupine Median High: implications for the formation of non-volcanic rifted margins, *J. geol. Soci. Lond.,* **161**(5), 783–798.

Sandwell, D.T. & Smith, W.H., 1997. Marine gravity anomaly from Geosat and ERS 1 satellite altimetry, *J. geophys. Res.,* **102**(B5), 10 039–10 054.

Sclater, J. & Christie, P., 1980. Continental stretching: an explanation of the post-mid-Cretaceous subsidence of the central North Sea Basin, *J. geophys. Res.,* **85**(B7), 3711–3739.

Scrutton, R., 1986. The geology, crustal structure and evolution of the Rockall Trough and the Faeroe-Shetland Channel, *Proc. R. Soc. Edinburgh,* **88B,** 7–26.

Shannon, P., 1991. The development of Irish offshore sedimentary basins, *J. geol. Soc. Lond.,* **148,** 181–189.

Shannon, P., 1995. Permo-Triassic development of the Celtic Sea region, offshore Ireland, in *Permian and Triassic Rifting in Northwest Europe,* Vol. 91, pp. 215–237, eds Boldy, S., Geological Society of London, Special Publications.

Shannon, P., Jacob, A.B., O'Reilly, B., Hauser, F., Readman, P. & Makris, J., 1999. Structural setting, geological development and basin modelling in the Rockall Trough, in *Petroleum Geology of North West Europe: Proceedings of the Fifth Conference,* Vol. 5, pp. 421–431, eds Fleet, A. & Boldy, S., Geological Society.

Sinclair, I., Shannon, P., Williams, B., Harker, S. & Moore, J., 1994. Tectonic control on sedimentary evolution of three North Atlantic borderland Mesozoic basins, *Basin Res.,* **6,** 193–218.

Smythe, D., 1989. Rockall Trough—Cretaceous or Late Paleozoic? *Scott. J. Geol.,* **25**(1), 5–43.

Srivastava, S., Verhoef, J. & Macnab, R., 1988a. Results from a detailed aeromagnetic survey across the northeast Newfoundland margin, Part I: spreading anomalies and the ocean-continent boundary, *Mar. Petrol. Geol.,* **5,** 306–323.

Srivastava, S., Verhoef, J. & Macnab, R., 1988b. Results from a detailed aeromagnetic survey across the northeast Newfoundland margin, Part II: Early opening of the North Atlantic between the British Isles and Newfoundland, *Mar. Petrol. Geol.,* **5,** 324–336.

Srivastava, S., Roest, W., Kovacs, L., Oakey, G., Lévesque, S., Verhoef, J. & Macnab, R., 1990. Motion of Iberia since the Late Jurassic: Results from detailed aeromagnetic measurements in the Newfoundland Basin, *Tectonophysics,* **184**(3–4), 229–260.

Stoker, M., 1997. Mid to late Cenozoic sedimentation on the continental margin off NW Britain, *J. geol. Soc. Lond.,* **154,** 509–515.

Štolfovà, K. & Shannon, P., 2009. Permo-Triassic development from Ireland to Norway: basin architecture and regional controls, *Geol. J.,* **44,** 652–676.

Tucholke, B. & Sibuet, J.-C., 2007. Leg 210 synthesis: tectonic, magmatic and sedimentary evolution of the Newfoundland-Iberia rift, *Proc. Ocean Drill. Project Scient. Results,* **210,** 1–56.

Tucholke, B., Austin, J. & Uchupi, E., 1989. Crustal structure and rift-drift evolution of the Newfoundland basin, in *Extensional Tectonics and Stratigraphy of the North Atlantic Margins,* Vol. 46, Chap. 16, pp. 247–263, eds Tankard, A. & Balkwill, H., AAPG Memoir.

Tyrrell, S., Haughton, P. & Daly, J., 2007. Drainage reorganization during breakup of Pangea revealed by in-situ Pb isotopic analysis of detrical K-feldspar, *Geology,* **35**(1), 971–974.

van den Berg, R., Daly, J. & Salisbury, M., 2005. Seismic velocities of granulite-facies xenoliths from Central Ireland: implications for lower crustal composition and anisotropy, *Tectonophysics,* **407,** 81–99.

Vogt, U., Makris, J., O'Reilly, B., Hauser, F., Readman, P., Jacob, A.B. & Shannon, P., 1998. The Hatton basin and continental margin: crustal structure from wide-angle seismic and gravity data, *J. geophys. Res.,* **103**(B6), 12 545–12 566.

Warner, M., 1987. Seismic reflections from the Moho - the effect of isostasy, *Geophys. J. R. astr. Soc.,* **88**(2), 425–435.

Welford, J.K. & Hall, J., 2007. Crustal structure across the Newfoundland rifted continental margin from constrained 3-D gravity inversion, *Geophys. J. Int.,* **171,** 890–908.

White, R. & McKenzie, D., 1989. Magmatism at rift zones: the generation of volcanic continental margin and flood basalts, *Geophys. Res.,* **94,** 7685–7729.

White, R., Smith, L., Roberts, A., Christie, P., Kusznir, N. & the rest of the iSIMM Team, 2008. Lower-crustal intrusion on the North Atlantic continental margin, *Nature,* **452,** 460–464.

Whitmarsh, R., Langford, J., Buckley, J., Bailey, R. & Blundell, D., 1974. The crustal structure beneath the Porcupine Ridge as determined by explosion seismology, *Earth planet. Sci. Lett.,* **22,** 197–204.

Williams, H., 1984. Miogeoclines and suspect terranes of the Caledonian-Appalachian orogen: tectonic patterns in the North Atlantic region, *Can. J. Earth Sci.,* **21**(887–901).

Williams, H., 1995. *Geology of the Appalachian-Caledonian orogen in Canada and Greenland,* Geological Survey of Canada, Geology of Canada, no. 6.